Supplementary Figures for:

Title:

Amyloid-β plaque diversity across brain regions in Alzheimer's disease and its relation to major clinicopathological traits

Authors:

Antonia Neubauer[1,2,3], Paul Feyen[1,2], Susanna Pekrun [1,2], Sigrun Roeber[1,2], Viktoria Ruf [1,2], Felix L. Strübing[1,2], Jochen Herms[1,2,3]

Affiliations:
[1]*Institute of Neuropathology, LMU Medizin, Ludwig-Maximilians-Universität München, Munich, Germany*
[2]*German Center for Neurodegenerative Diseases (DZNE), Munich, Germany*
[3]*Munich Cluster for Systems Neurology (SyNergy), Munich, Germany*

Corresponding author:

Antonia.Neubauer@med.uni-muenchen.de

Table of contents

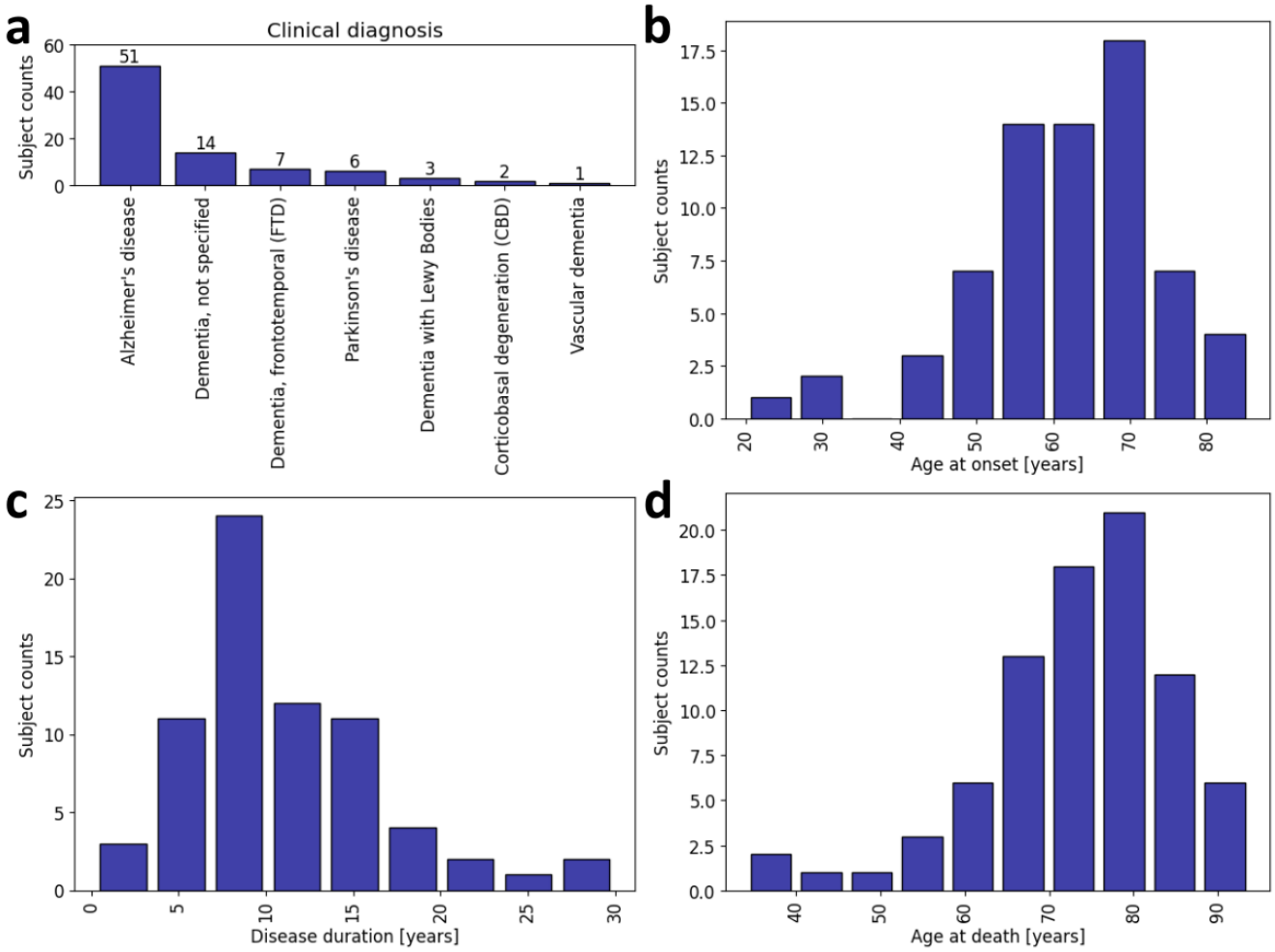

Fig. S1: *Overview of the study cohort*

Histograms show the distribution of clinical diagnoses, age at symptom onset, disease duration and age at death of the study cohort.

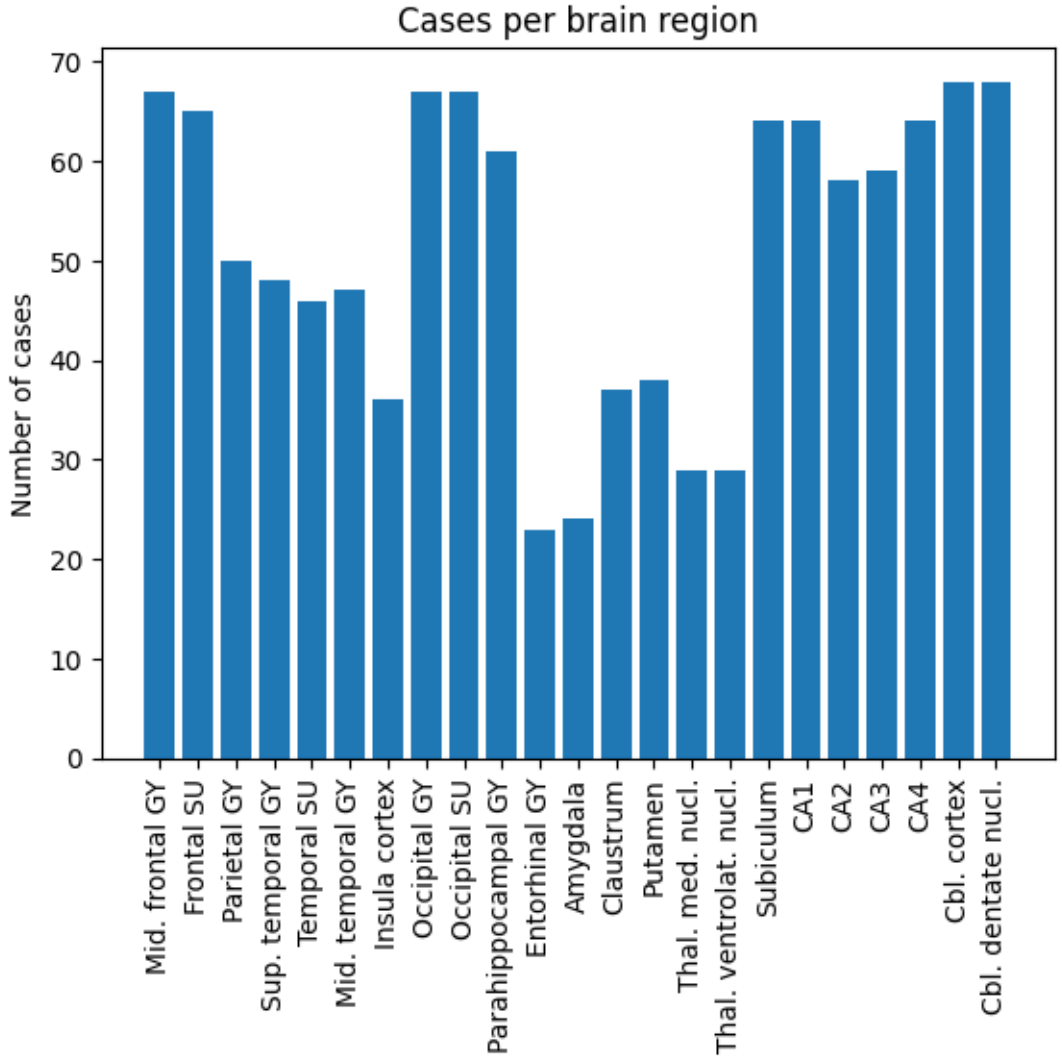

Fig. S2: *Staining availability*

Histogram of how many cases were available for each brain region. CA cornu ammonis (hippocampus), Cbl. cerebellum, GY gyrus, med. Medial, mid. middle, nucl. nucleus, SU sulcus, Sup. superior, Thal thalamus, ventrolat. Ventrolateral

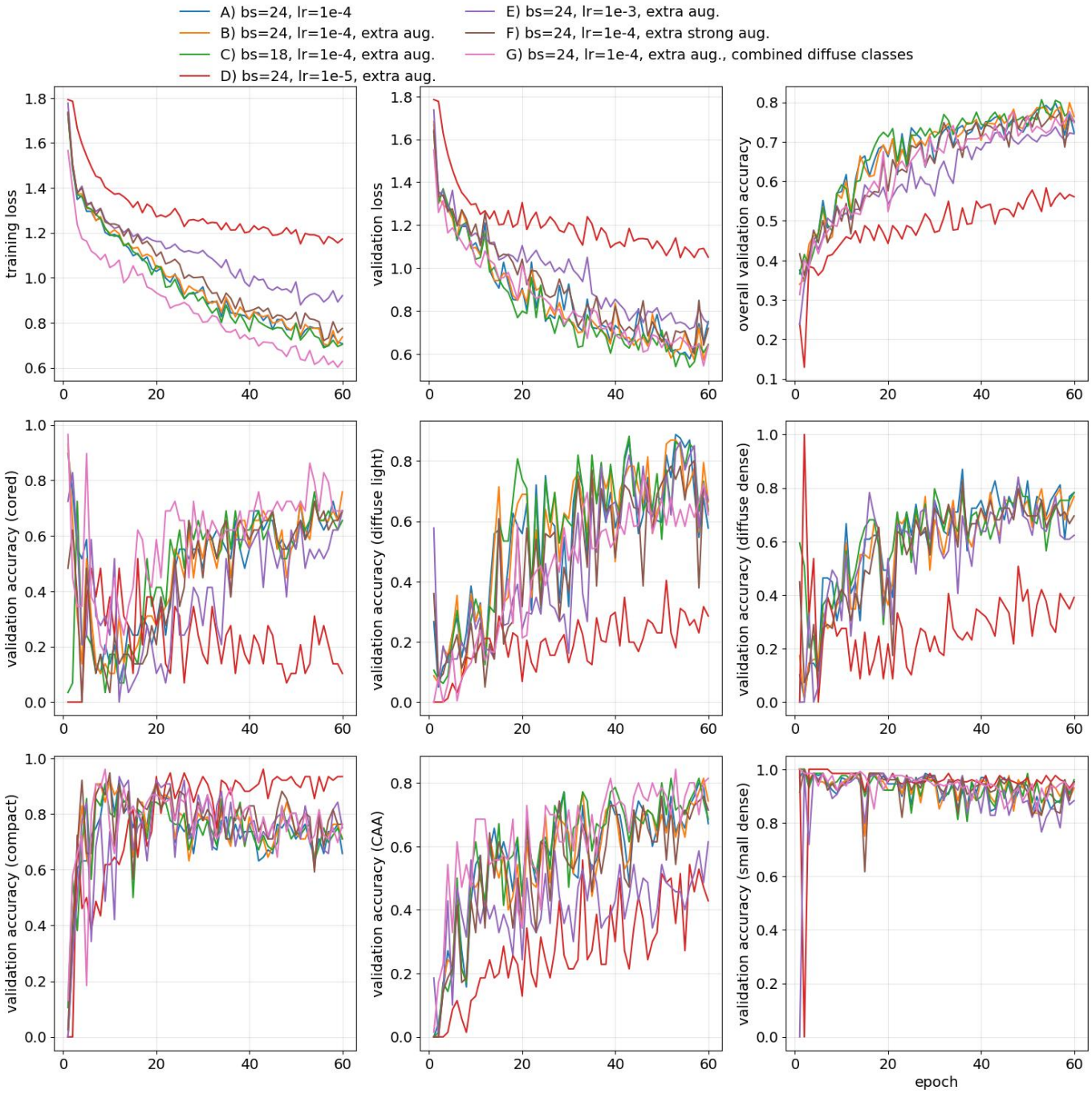

Fig. S3: *Convolutional neural network optimization*

General and class-wise model performances during training, tested on the validation set, which is not equal to the test set. The x-axis shows the number of epochs. Moderate data augmentation with torchvision (version 0.18.1) included random rotation, horizontal and vertical flip, color jitter (transforms.ColorJitter (brightness=0.1, contrast=0.1, saturation=0.1, hue=0.02)), and further low-grade geometric augmentations (transforms.RandomAffine (0, translate=(0.05, 0.05), scale=(0.95, 1.05), shear=10)). Extra data augmentation (extra aug.) means that underrepresented deposit classes, e.g. cored plaques and CAA, have a higher probability to pass additional data augmentation (transforms.ColorJitter (brightness=0.1, contrast=0.2, saturation=0.2, hue=0.02); transforms.RandomAffine (0, translate=(0.08, 0.08), scale=(0.9, 1.1), shear=10)) to increase the variability in minority classes. Strong data augmentation (strong aug.) included transforms.ColorJitter (brightness=0.2, contrast=0.2, saturation=0.2, hue=0.02) and transforms.RandomAffine (0, translate=(0.05, 0.05), scale=(0.9, 1.1), shear=12). In model G, the classes diffuse light and diffuse dense deposits were combined as one class, here shown in the central plot for diffuse light plaques. Finally, model A was selected for further application. Accuracy and recall are used interchangeably. aug. data augmentation, bs batch size, lr learning rate

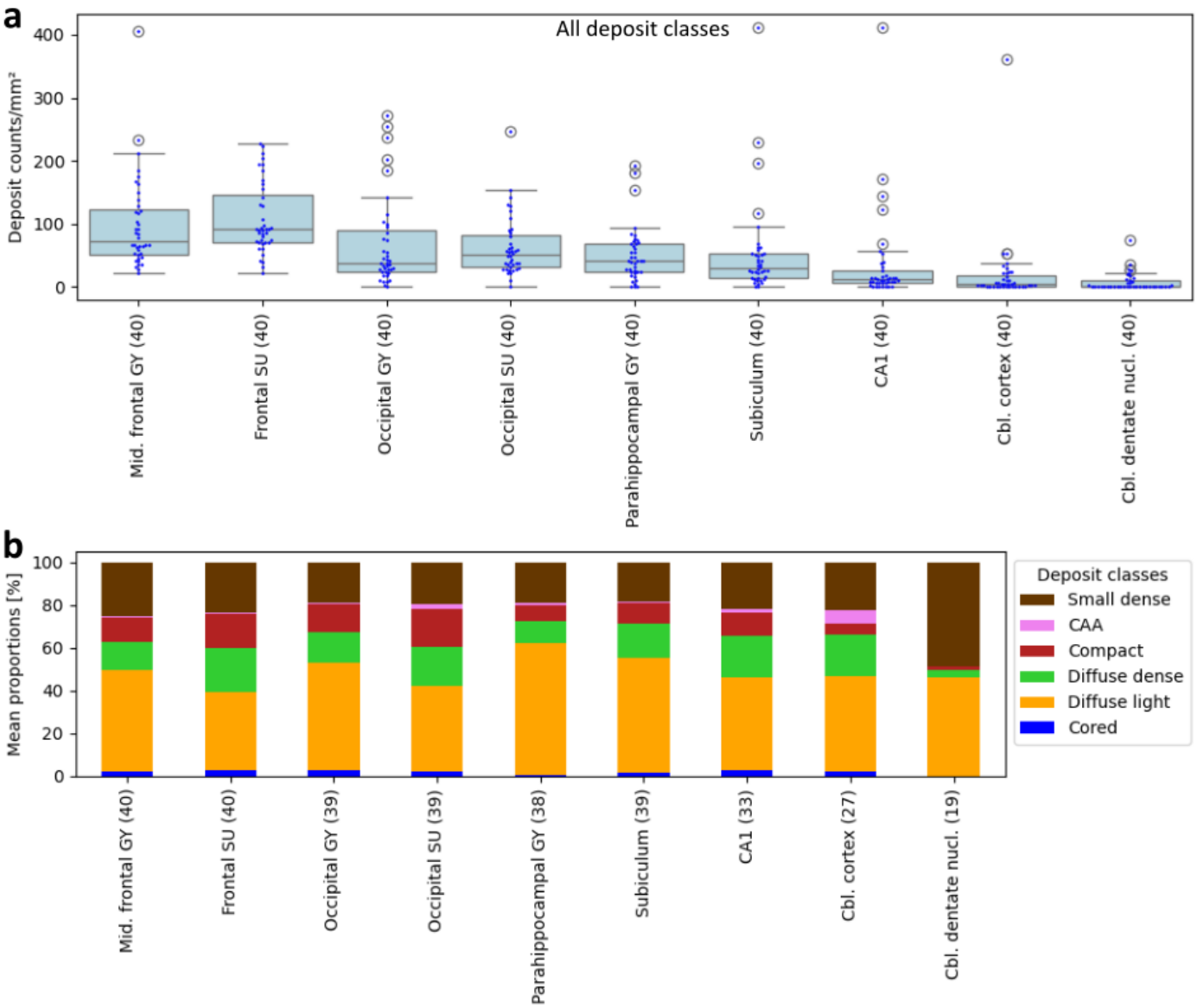

Fig. S4: *Aβ deposit classes across regions with a data subset*

These plots correspond to the main Fig. 3a and b but with a subset of 40 subjects that have complete data for the nine brain regions listed here. The idea is to get a visual impression if there is a bias in the whole cohort because of the missing data points. (a) Deposit counts per mm² summing up all deposit classes per region. (b) Mean proportions of deposit classes [%] in each region. The numbers in brackets behind region names indicate how many cases are included in the above plot. Numbers in plot b can be lower as proportions of plaques cannot be calculated in images with zero detected deposits. CAA cerebral amyloid angiopathy, Cbl. cerebellum, GY gyrus, med. medial, mid. middle, nucl. nucleus, SU sulcus

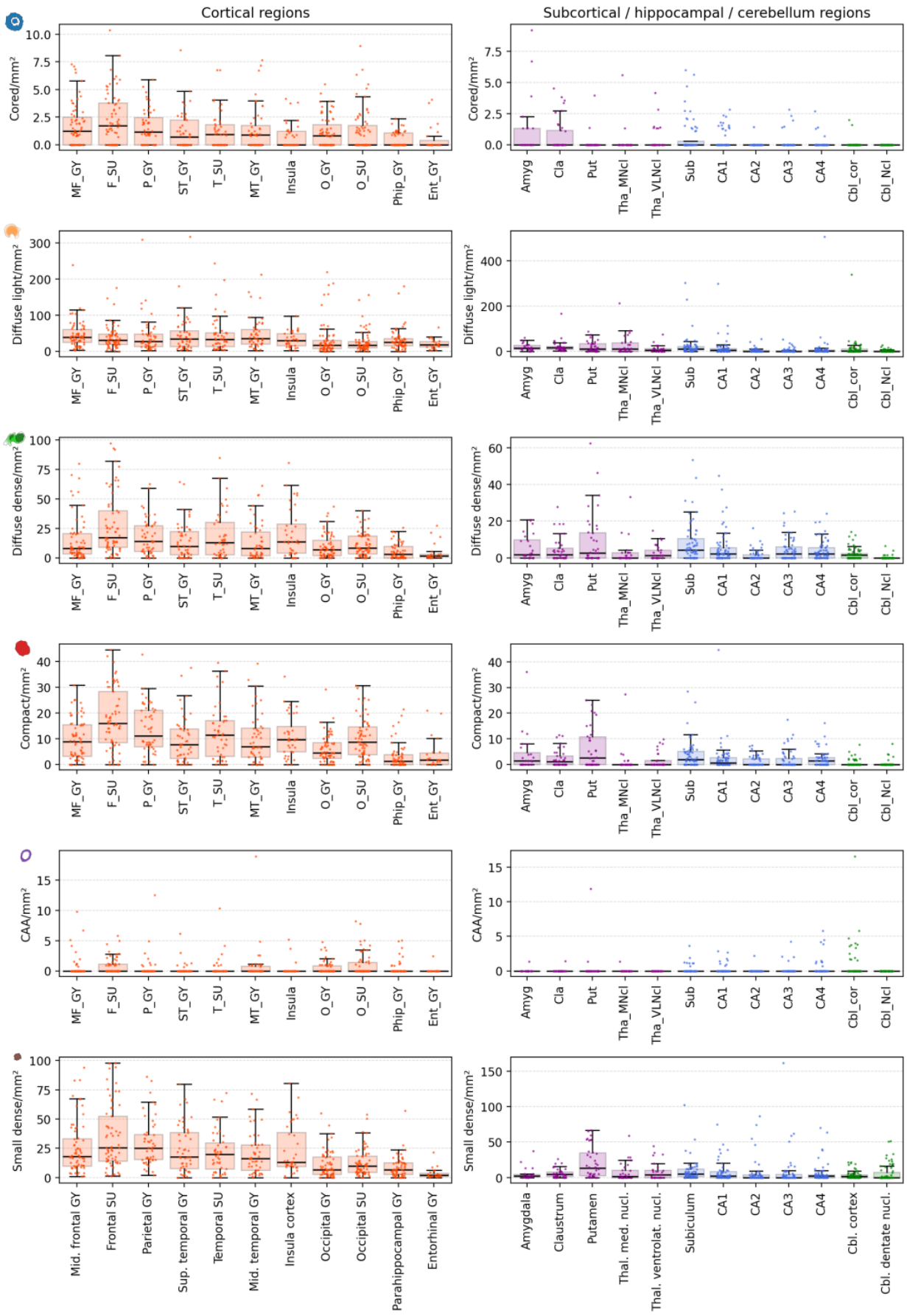

Fig. S5: *Aβ deposit counts per mm² separately for each deposit class and brain region*

Cortical regions are shown on the left side, non-cortical regions on the right. Amyg amygdala, CAA cerebral amyloid angiopathy, Cbl cerebellum, Cla claustrum, cor cortex, Dentncl dentate nucleus, Ent entorhinal, F frontal, GY gyrus,

med. medial, mid. middle, MF middle frontal, MNcl medial nucleus, MT middle temporal, nucl. nucleus, O occipital, P parietal, Phip parahippocampal, Put putamen, ST superior temporal, SU sulcus, Sub subiculum, Sup. superior, T temporal, Thal thalamus, vetrolat. Ventrolateral, VlNcl ventrolateral nucleus

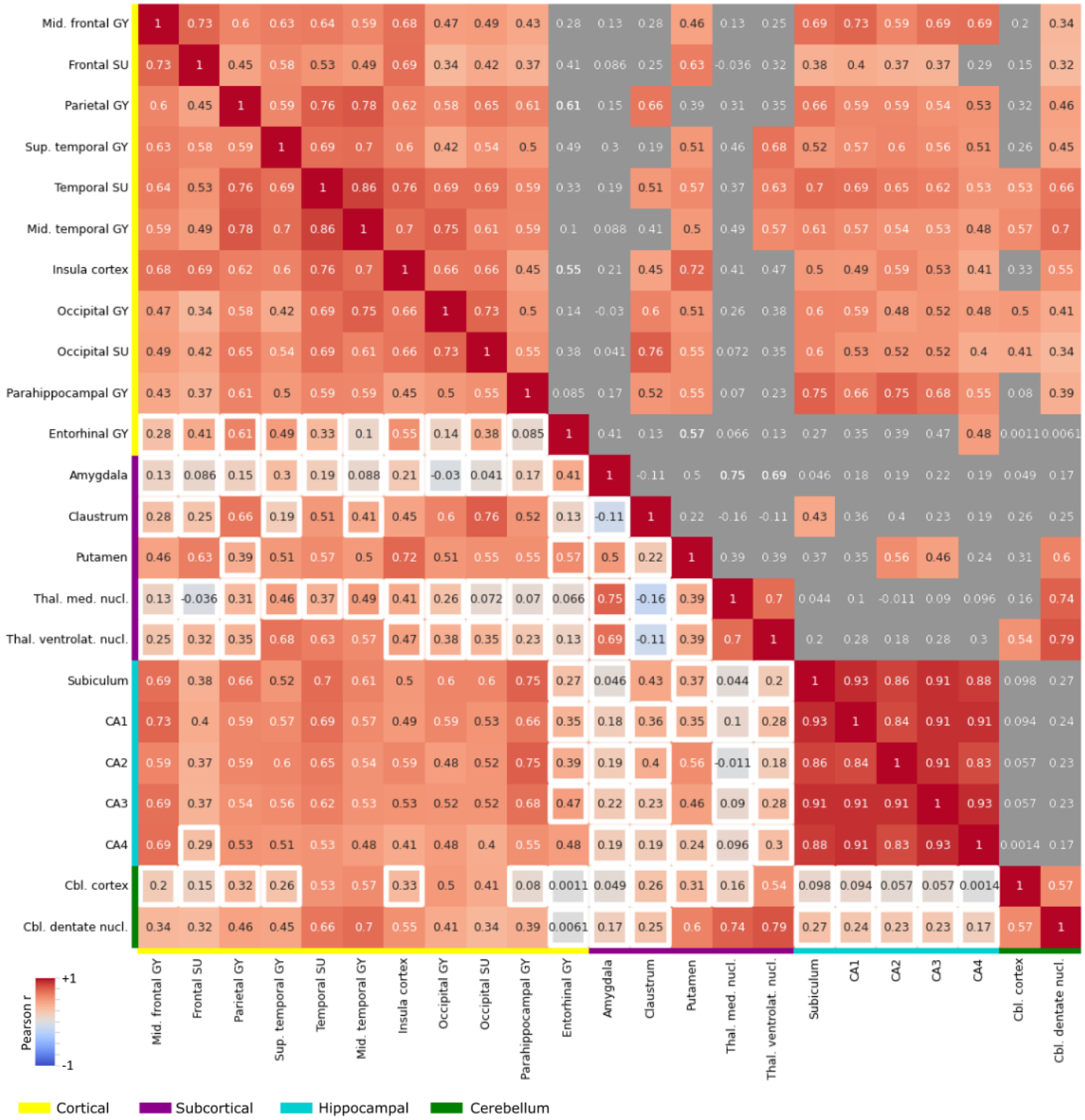

Fig. S6: *Pearson correlation between regional deposit counts of all classes together (/mm²)*

This Fig. matches the large triangle heatmap in main Fig. 3c. Non-significant correlation coefficients are shown with gray background color in the upper half or white frame in the lower half. Corresponding false discovery rate corrected p-values are presented in the SFig. below. CA cornu ammonis (hippocampus), Cbl. cerebellum, GY gyrus, med. medial, mid. middle, nucl. nucleus, SU sulcus, Sup. superior, Thal thalamus, ventrolat. ventrolateral

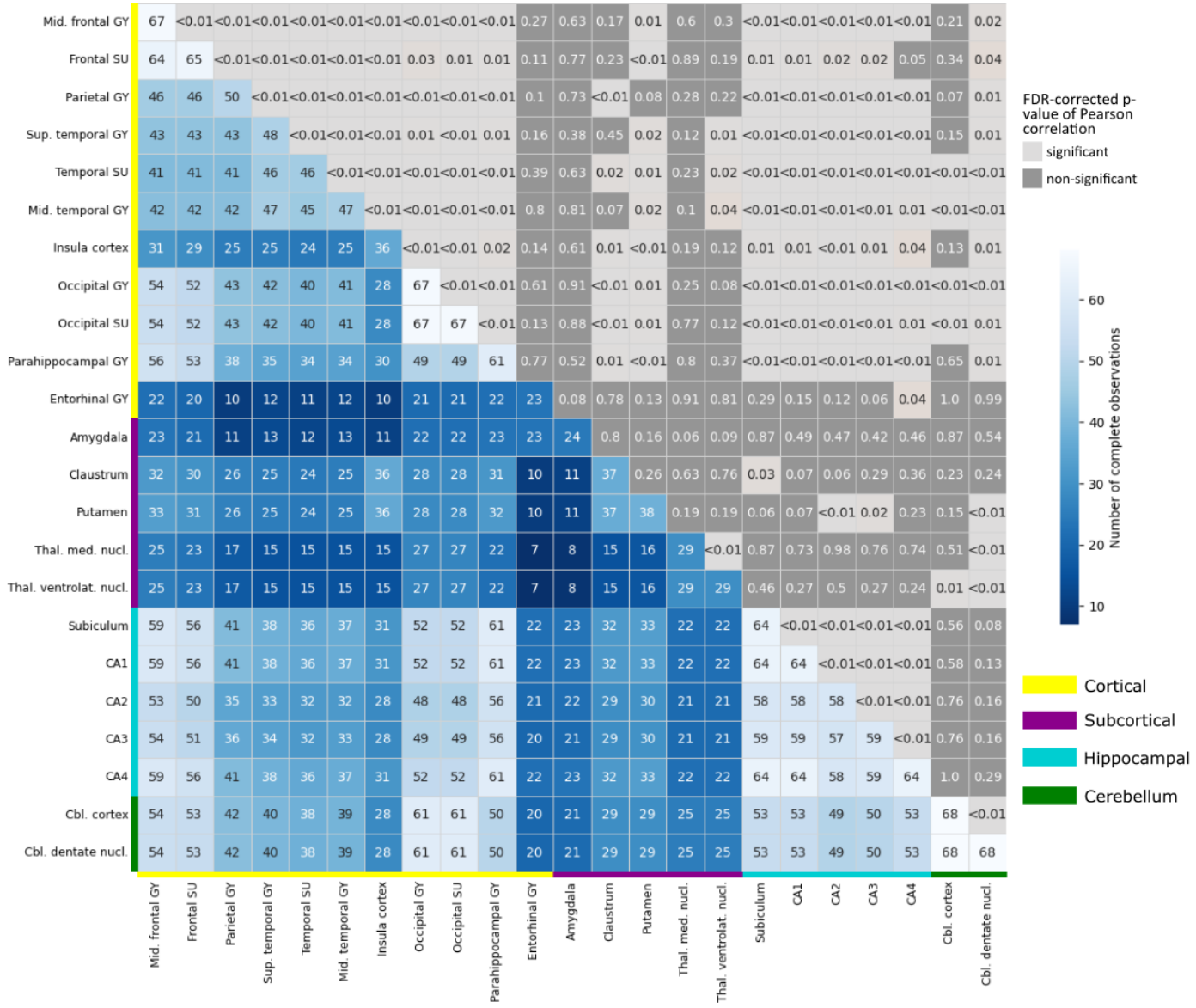

Fig. S7: *P-values and n of the above Pearson correlation analysis*

Upper half: False discovery rate corrected p-values corresponding to the correlation analysis of Aß deposit counts between brain regions in the previous figure. Lower half: Number of available observations per region combination. CA cornu ammonis (hippocampus), Cbl. cerebellum, GY gyrus, med. medial, mid. middle, nucl. nucleus, SU sulcus, Sup. superior, Thal thalamus, ventrolat. ventrolateral

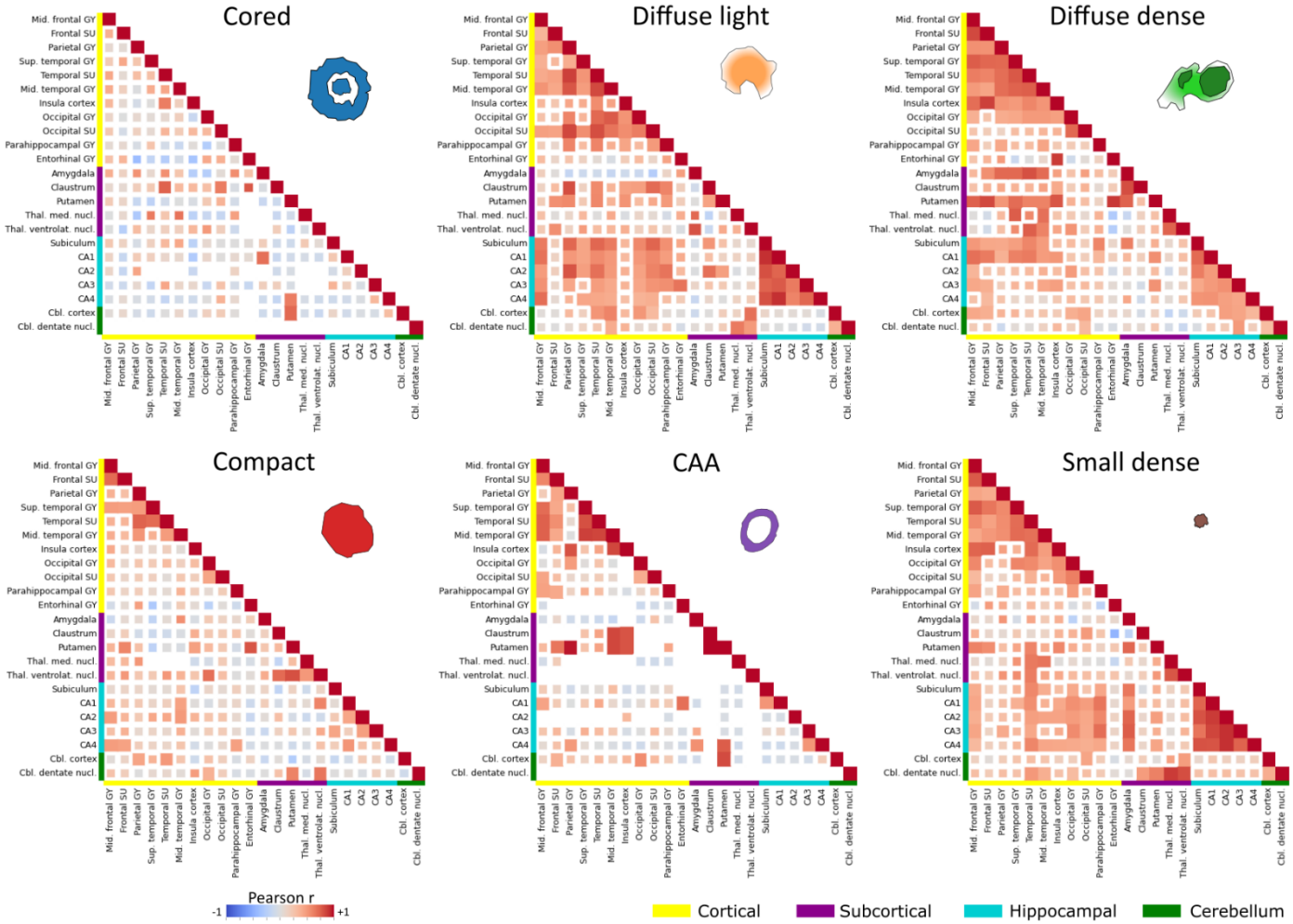

Fig. S8: *Class-wise Aß plaque correlations between brain regions*

The heatmaps show Pearson correlation coefficients between brain regions regarding plaque counts per mm² for each Aß deposit class separately. Non-significant correlations are labeled with a white frame. Completely white cells indicate less than three datapoints for this correlation. The subplots for diffuse light, diffuse dense and small dense plaques are also shown in main Fig. 3c. CA cornu ammonis (hippocampus), Cbl. cerebellum, GY gyrus, med. medial, mid. middle, nucl. nucleus, SU sulcus, Sup. superior, Thal thalamus, ventrolat. ventrolateral

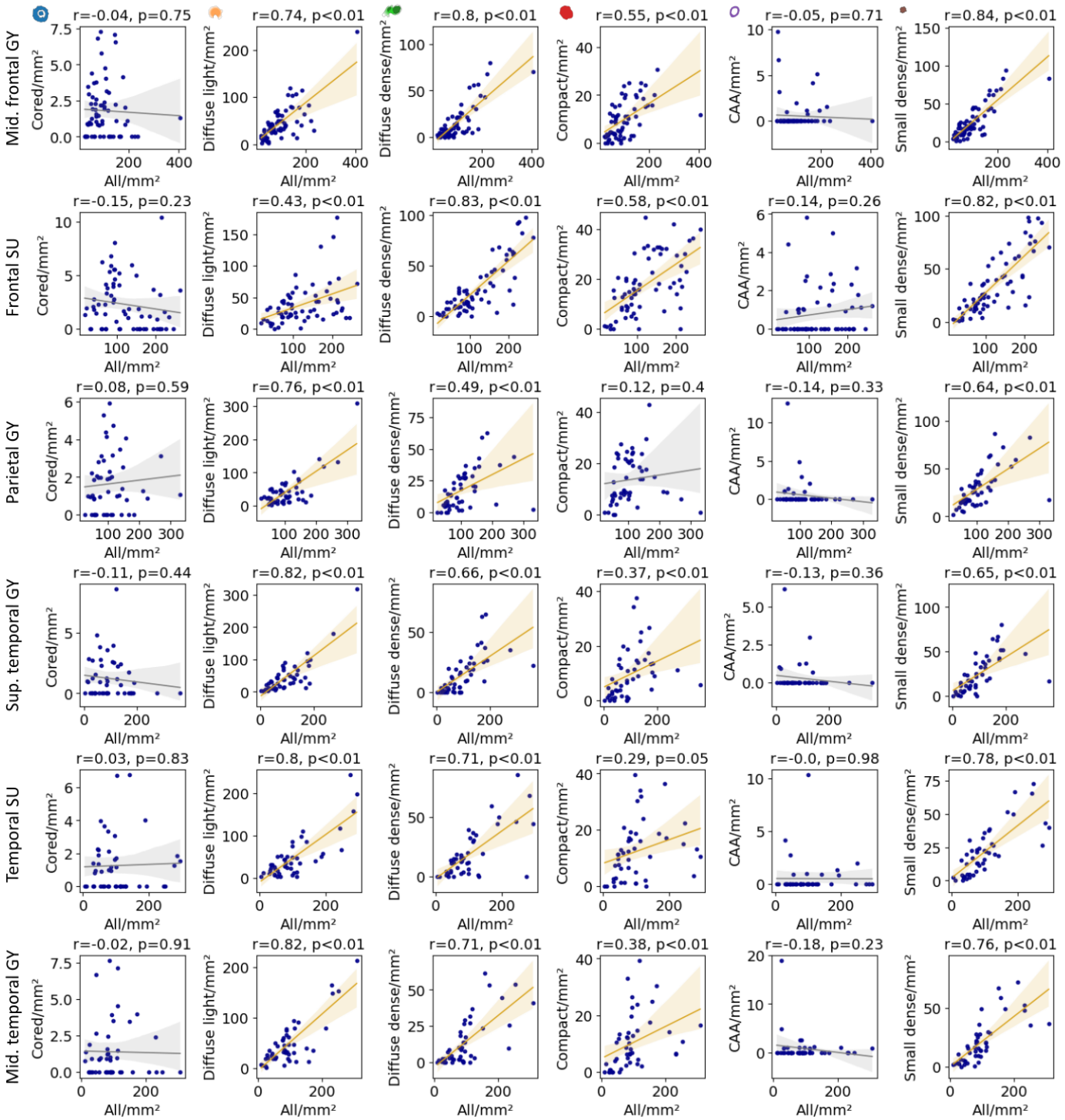

Fig. S9: *Regional associations between Aß deposit classes and total Aß load*

Pearson correlation coefficients r between deposit classes (counts/mm²) and total Aß plaque loads (All/mm²) for each cortical brain region separately. Significant correlations are shown with yellow regression lines, non-significant correlations are grayed out (without false discovery rate correction). This Fig. is continued in the following Fig. CAA cerebral amyloid angiopathy, GY gyrus, Mid. middle, SU sulcus, Sup. superior

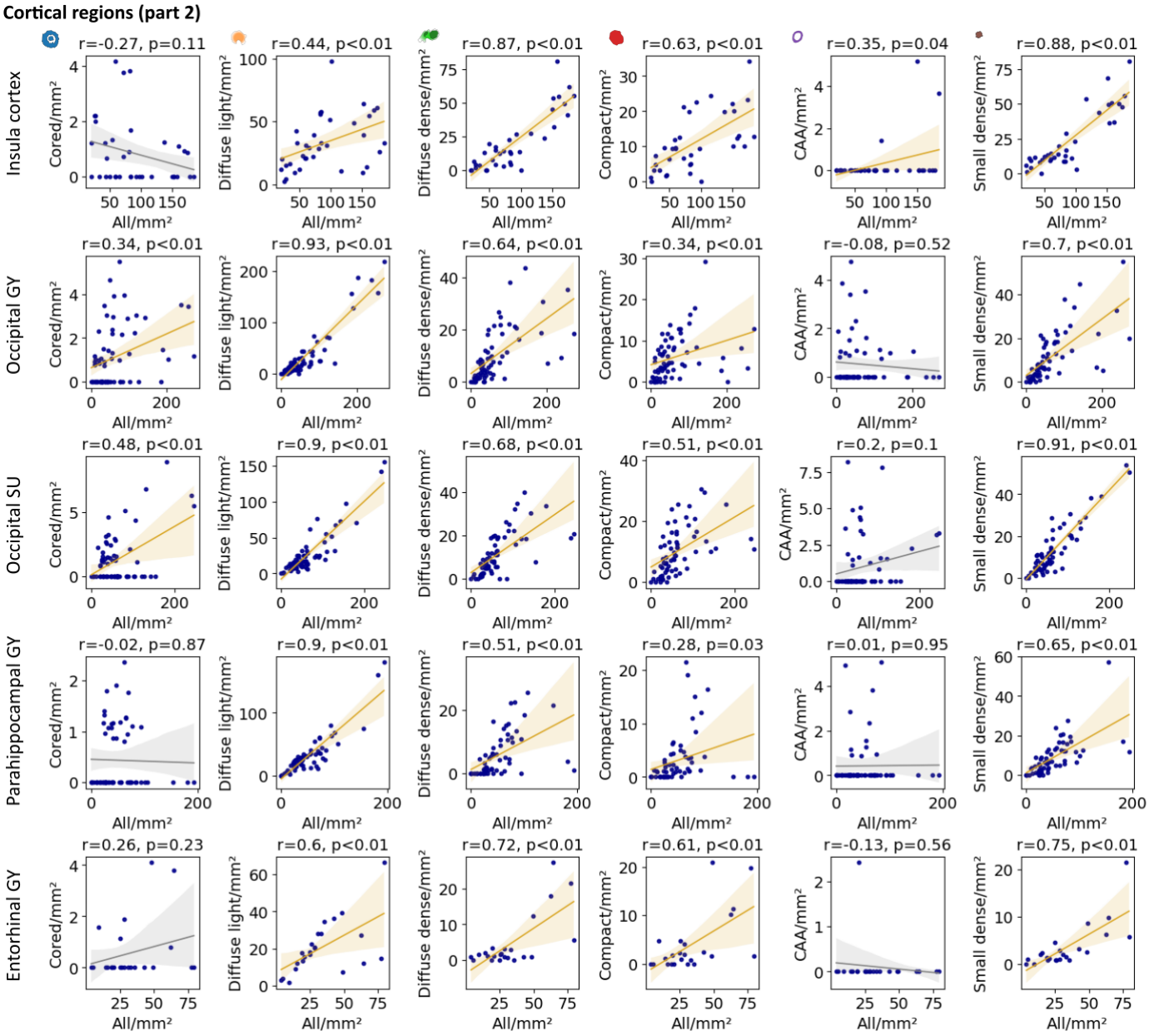

Fig. S10: *This Fig. continues the preceding Fig.*

Pearson correlation coefficients r between deposit classes (counts/mm²) and total Aβ plaque loads (All/mm²) for each cortical brain region separately. Significant correlations are shown with yellow regression lines, non-significant correlations are grayed out (without false discovery rate correction). CAA cerebral amyloid angiopathy, GY gyrus, Med. medial, SU sulcus, Sup. superior

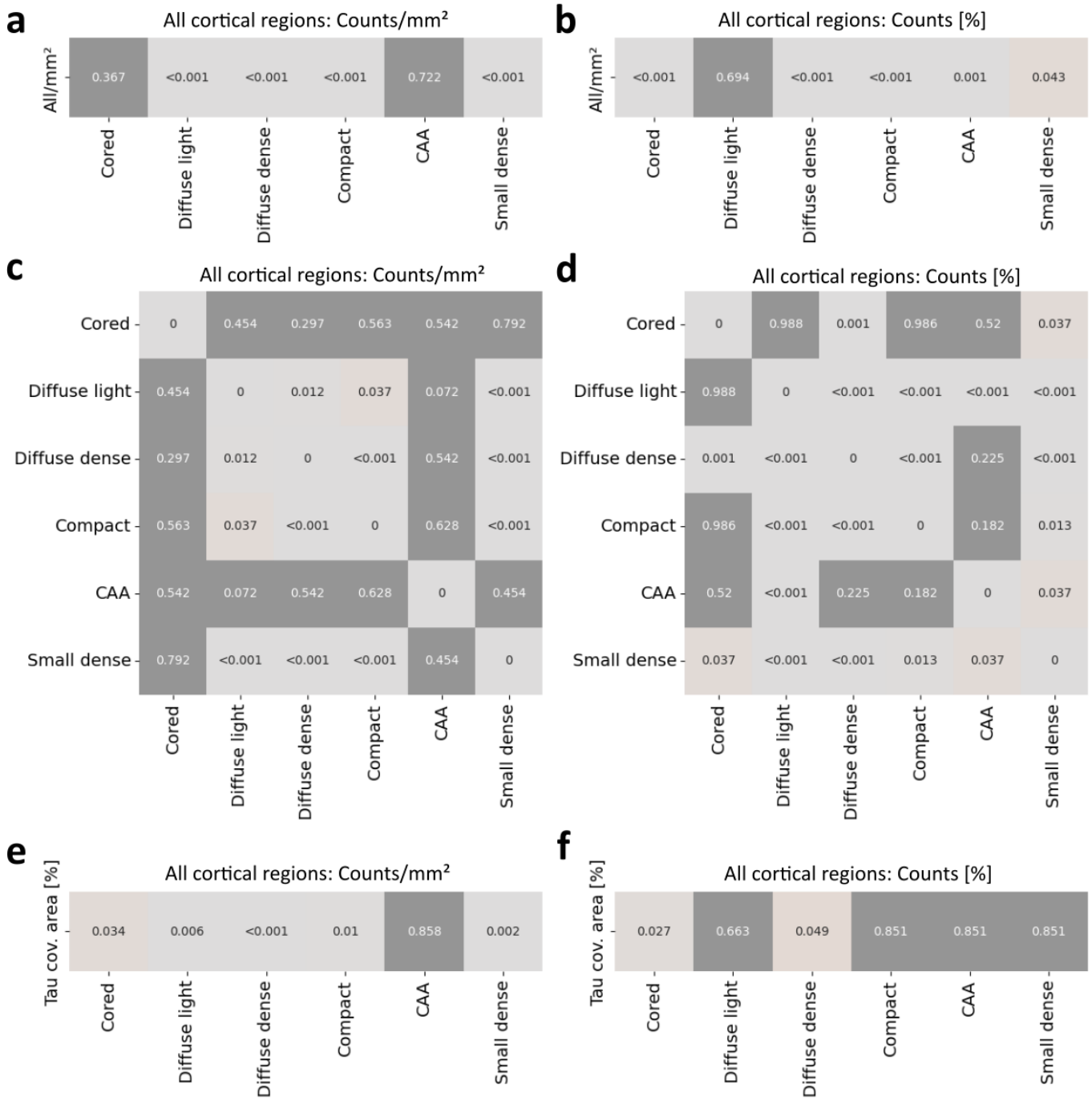

Fig. S11: *False discovery rate corrected p-values of Pearson correlation analyses*

Significant p-values are highlighted in light gray. (a) P-values for main Fig. 4a, correlating cortical plaque counts (/mm²) with the overall Aß plaque load. (b) P-values for main Fig. 4c, correlating the proportions of cortical plaque loads (%) with the overall Aß plaque load. (c) P-values for main Fig. 4e, correlating counts of plaque classes (/mm²) across cortical regions. (d) P-values for main Fig. 4g, correlating proportional loads of plaque classes (%) across cortical regions. (e) P-values for main Fig. 5a, correlating the entorhinal tau load (% of covered area) with the counts of Aß plaques across cortical regions. (f) P-values for Fig. S11a, correlating the entorhinal tau load (% of covered area) with the proportional load of Aß deposit classes (%) across cortical regions. CAA cerebral amyloid angiopathy, cov. covered

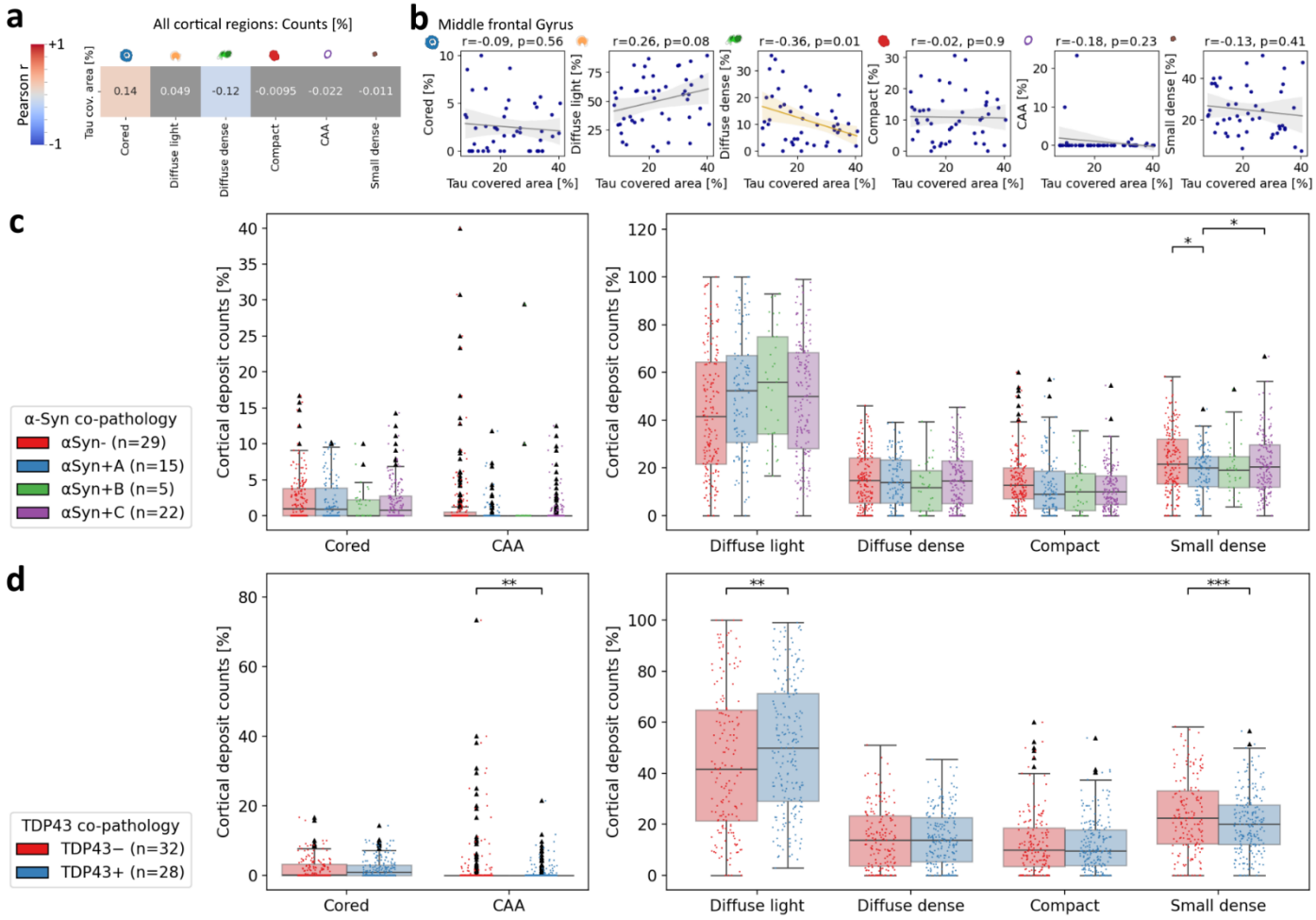

Fig. S12: *Associations between Aß deposit classes and other protein deposits*

This Fig. repeats the analysis from main Fig. 5, but with proportional Aß plaque loads instead of counts per mm². (a) Pearson correlation coefficients r across cortical regions between the tau covered area in the entorhinal cortex (%) and proportions of individual deposit classes. Statistics were corrected for individual region names by linear regression; the significance level was set to <0.05 after false discovery rate correction. Non-significant correlations are grayed out. (b) Scatterplots illustrate the Pearson correlation analysis in parallel to (a) with tau covered area in the entorhinal cortex on the x-axis and Aß deposit proportions in the middle frontal gyrus on the y-axis. (c) Comparison of cortical Aß deposit classes between aSyn co-pathology groups. (d) Comparison between TDP43 co-pathology groups. In (c) and (d), groups were compared with multiple linear regression correcting for ApoE genotype, age at death, sex, region names, and false discovery rate correction for multiple testing. The numbers (n=) indicate how many cases were included in the scatter dots. In the linear regression analyses, individual cases with incomplete data for the covariates were excluded. CAA cerebral amyloid angiopathy, aSyn- no aSyn co-pathology, aSyn+A amygdala predominant aSyn co-pathology, aSyn+B brainstem predominant aSyn co-pathology, aSyn+C cortical disseminated aSyn co-pathology

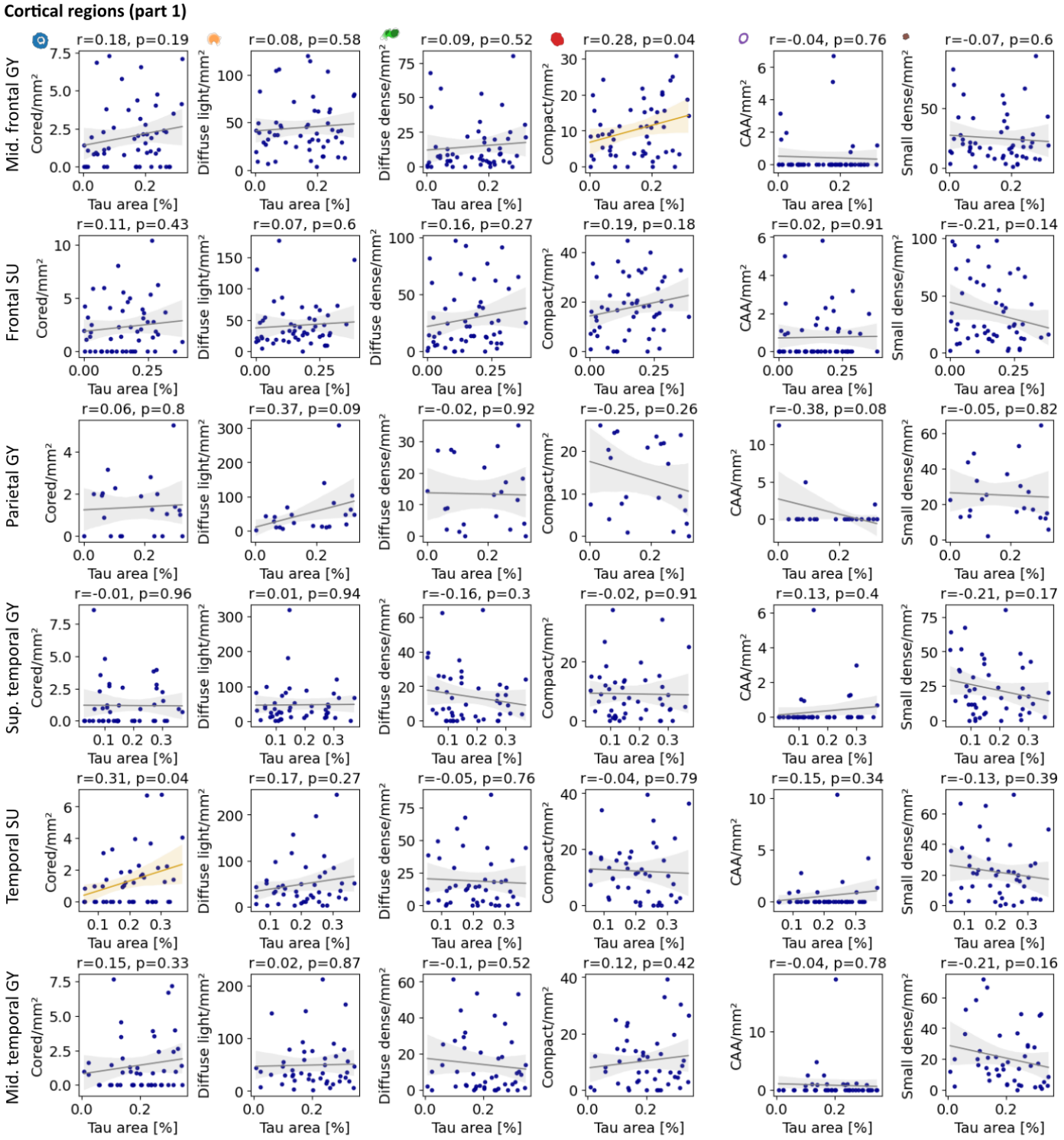

Fig. S13: *Correlations between Aß and tau load within cortical regions*

Scatterplots illustrate the Pearson correlation analysis between the tau covered area (%) of the specified brain region (row) and the density of each plaque class (/mm²) in the same region. Significant correlations are shown with yellow regression lines, non-significant correlations are grayed out (without false discovery rate correction). This Fig. is continued in the following Fig. CAA cerebral amyloid angiopathy, GY gyrus, Mid. middle, SU sulcus, Sup. superior

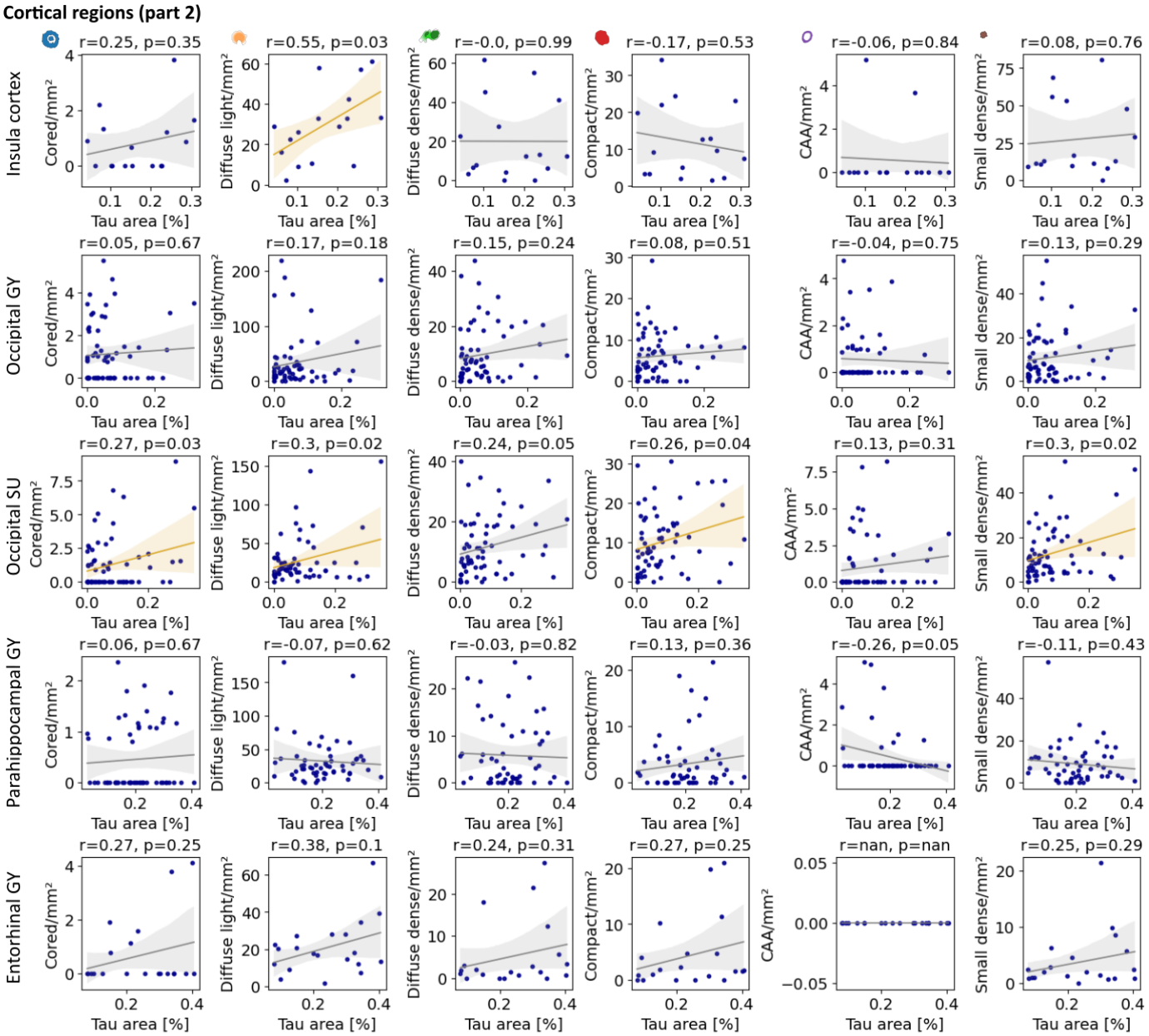

Fig. S14: *This Fig. continues the preceding Fig.*

Correlations between Aβ and tau load within cortical regions. Scatterplots illustrate the Pearson correlation analysis between the tau covered area (%) of the specified brain region (row) and the density of each plaque class (/mm²) in the same region. Significant correlations are shown with yellow regression lines, non-significant correlations are grayed out (without false discovery rate correction). CAA cerebral amyloid angiopathy, GY gyrus, Med. medial, SU sulcus, Sup. superior

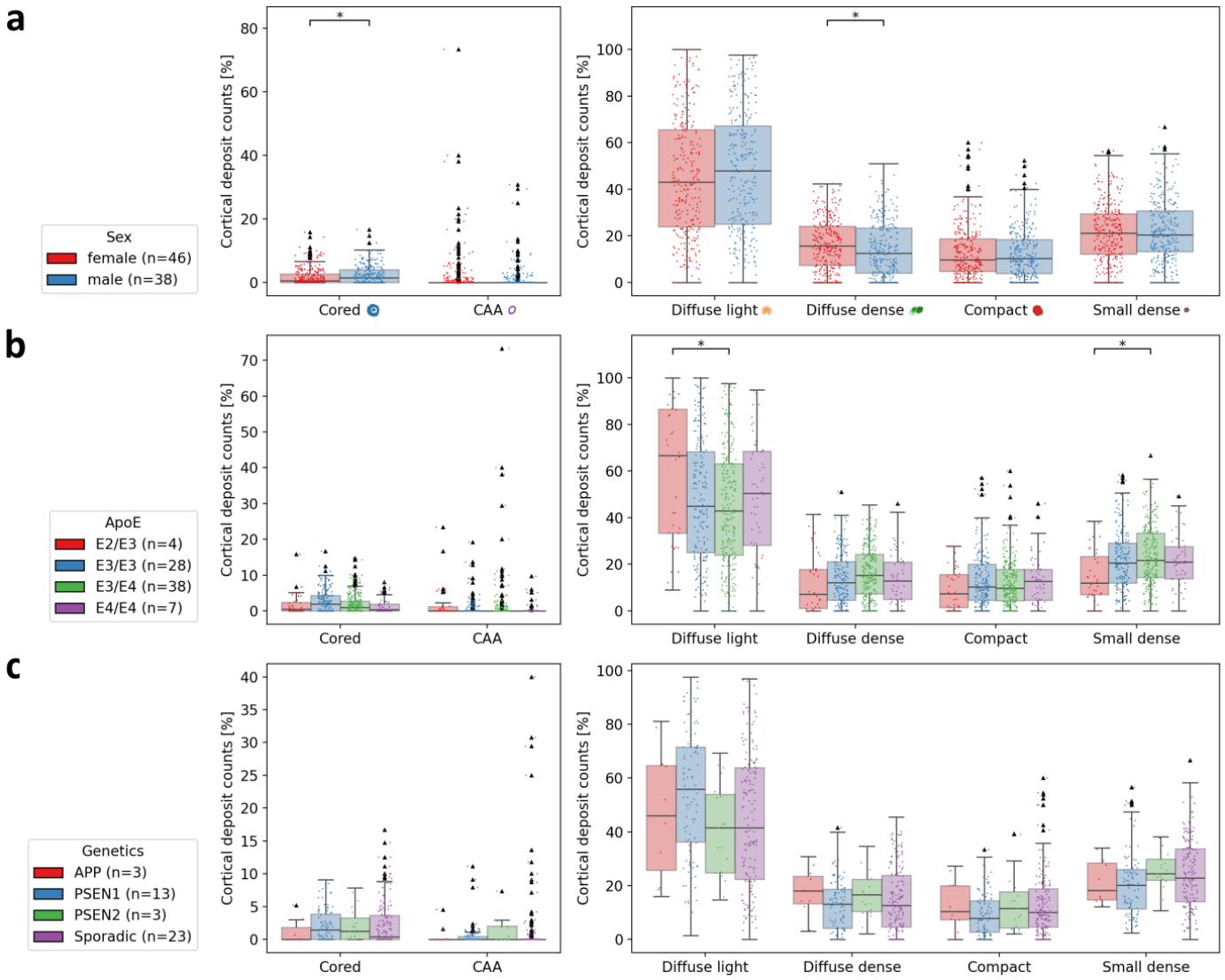

Fig. S15: *Associations between Aβ deposit classes and genetic factors*

This Fig. repeats the analysis from main Fig. 6, but with proportional Aβ plaque loads instead of counts per mm². (a) Comparison of cortical Aβ deposit classes between female and male Alzheimer's disease (AD) cases. Groups were compared with multiple linear regression correcting for ApoE genotype, age at death, and region names. (b) Comparison between ApoE genotypes. Groups were compared with multiple linear regression correcting for sex, age at death, and region names. (c) Comparison between familial and sporadic Alzheimer's disease cases. Groups were compared with multiple linear regression correcting for sex, ApoE genotype, and region names. Sporadic cases were defined as AD with a reported age of onset >65 years and an inconspicuous whole genome sequencing for AD-related variants. In (a), (b) and (c), p-values were corrected for multiple testing by respective false discovery rate correction. The numbers (n=) indicate how many cases were included in the scatter dots. In the linear regression analyses, individual cases with incomplete data for the covariates were excluded. CAA cerebral amyloid angiopathy

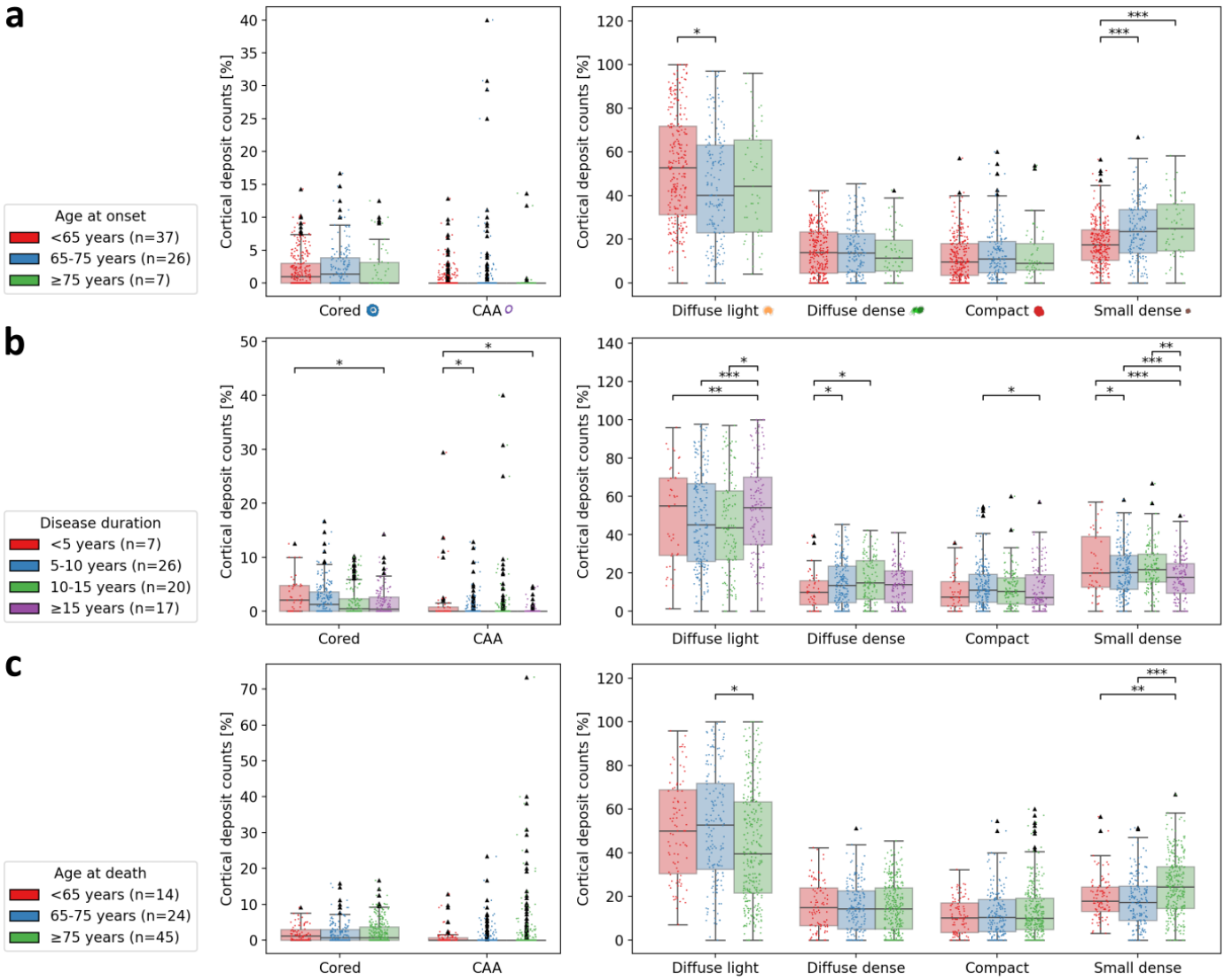

Fig. S16: *Associations between Aβ deposit classes and age*

This Fig. repeats the analysis from main Fig. 7, but with proportional Aβ plaque loads instead of counts per mm². (a) Comparison of cortical Aβ deposit class densities between early, middle-aged and late onset Alzheimer's disease (AD) cases. Groups were compared with multiple linear regression correcting for ApoE genotype, sex, and region names. (b) Comparison between different disease duration groups. Groups were compared with multiple linear regression correcting for sex, ApoE genotype, age at death, and region names. (c) Comparison between three groups with varying age at death. Groups were compared with multiple linear regression correcting for sex, ApoE genotype, and region names. In (a), (b) and (c), p-values were corrected for multiple testing by respective false discovery rate correction. The numbers (n=) indicate how many cases were included in the scatter dots. In the linear regression analyses, individual cases with incomplete data for the covariates were excluded. CAA cerebral amyloid angiopathy

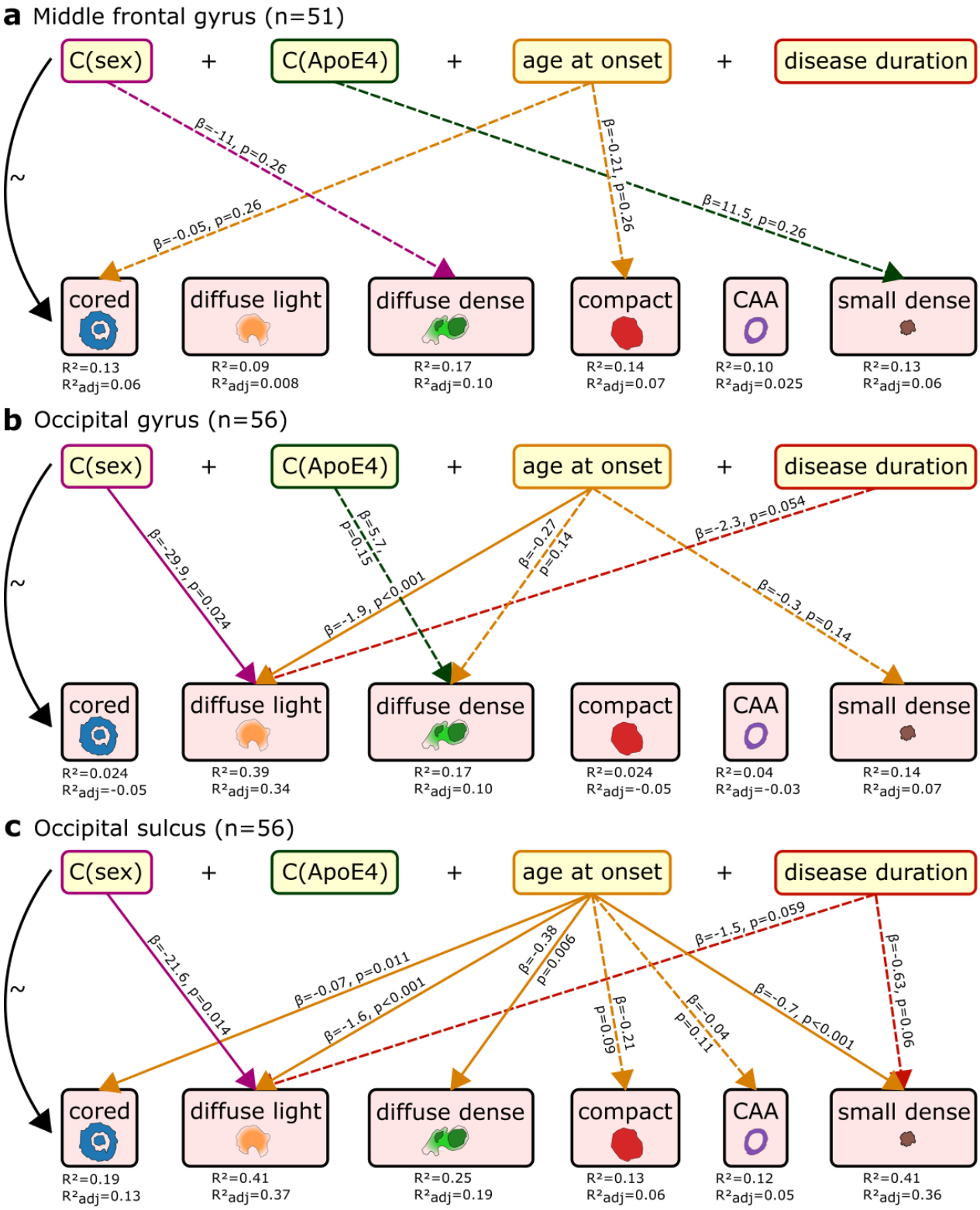

Fig. S17: *Integrative analysis of potential Aß plaque composition determinants for exemplary brain regions*

To investigate the associations of various factors (upper line in yellow) with densities (counts/mm²) of the six deposit classes (lower line in red), a multiple linear regression model was created for each deposit class separately for three brain regions (a, b, c). Sex (female vs. male), ApoE4 (no E4 vs. at least one E4 allele), age at onset, and disease duration were independent factors and the deposit classes were the dependent variables, respectively. C() indicates categorical variables. Significant effects after correction for false discovery rate (FDR) due to multiple testing are indicated with solid arrow lines, and associations that were only significant before FDR correction are labeled with dashed lines. Adj. adjusted, CAA cerebral amyloid angiopathy